Fractionation and fluxes of metals and radionuclides during the recycling process of phosphogypsum wastes applied to mineral CO_2 sequestration

M. Contreras [a], R. Pérez-López [b], M.J. Gázquez [a], V. Morales-Flórez [c,d], A. Santos [e], L. Esquivias [c,d], J.P. Bolívar [a,*]

[a] Department of Applied Physics, University of Huelva, Campus 'El Carmen', 21071 Huelva, Spain
[b] Department of Geology, University of Huelva, Campus 'El Carmen', 21071 Huelva, Spain
[c] Institute of Materials Science of Seville (CSIC-US), Av. Américo Vespucio, 49, 41092 Seville, Spain
[d] Department of Condensed Matter Physics, University of Seville, Av. Reina Mercedes, 41012 Seville, Spain
[e] Department Earth Sciences, University of Cádiz, Campus del Río San Pedro, Av. República Saharaui, 11510 Puerto Real, Spain

ABSTRACT

The industry of phosphoric acid produces a calcium-rich by-product known as phosphogypsum, which is usually stored in large stacks of millions of tons. Up to now, no commercial application has been widely implemented for its reuse because of the significant presence of potentially toxic contaminants. This work confirmed that up to 96% of the calcium of phosphogypsum could be recycled for CO_2 mineral sequestration by a simple two-step process: alkaline dissolution and aqueous carbonation, under ambient pressure and temperature. This CO_2 sequestration process based on recycling phosphogypsum wastes would help to mitigate greenhouse gasses emissions. Yet this work goes beyond the validation of the sequestration procedure; it tracks the contaminants, such as trace metals or radionuclides, during the recycling process in the phosphogypsum. Thus, most of the contaminants were transferred from raw phosphogypsum to portlandite, obtained by dissolution of the phosphogypsum in soda, and from portlandite to calcite during aqueous carbonation. These findings provide valuable information for managing phosphogypsum wastes and designing potential technological applications of the by-products of this environmentally–friendly proposal.

1. Introduction

Industrial production of fertilisers from phosphate rock ore by the wet process produces a gypsum-rich by-product called phosphogypsum (*PG*, $CaSO_4 \cdot 2H_2O$). It is generated in the production of phosphoric acid (H_3PO_4) during the acid attack of apatite (mainly fluorapatite, $Ca_5(PO_4)_3F$) with sulphuric acid (H_2SO_4) (Rutherford et al., 1994). The chemical reaction of the industrial process can be written as follows:

$$Ca_5(PO_4)_3F + 5H_2SO_4 + 10H_2O$$
$$\leftrightarrow 3H_3PO_4 + 5(CaSO_4 \cdot 2H_2O) + HF \quad (1)$$
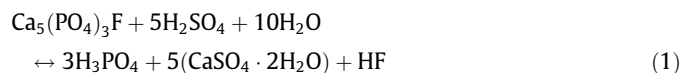
Worldwide phosphogypsum production is estimated to be around 280 Mt per year (Yang et al., 2009). However, only 15% of the phosphogypsum is recycled (Kim, 2010) because of existing contaminants, such as organic substances, metals and other potentially toxic elements and natural radionuclides from the ^{238}U decay

series (Mas et al., 2006; Pérez-López et al., 2007). The remaining 85% is often stored in large stacks in areas close to fertiliser plants (Tayibi et al., 2009). Spanish phosphoric acid production began in the city of Huelva (SW Spain) in 1968, and since then the *PG* waste has been slurried with water, pumped out of the fertiliser plant by a pipe system and then dumped on a nearby disposal site in the salt-marshes of the Tinto River (1200 ha containing about 120 Mt) without any commercial application (Bolívar et al., 2009a, 1995). The proximity of the waste to Huelva, less than 1 km away, is an important concern because of its alleged implications for the health of the local population of roughly 150,000 inhabitants. After looking unsuccessfully for sustainable solutions to the stockpiling of wastes, the fertiliser plant ceased dumping phosphogypsum in December 2010. However, the waste piles still remain in the area without an apparent solution. The urgent need to perform the current study is related to the great social interest in an action plan proposing solutions to the problem of the phosphogypsum stacks.

The main restrictions on reusing *PG* are related to its relatively high content of radionuclides and metallic elements, and evidence

---

* Corresponding author.
  E-mail address: bolivar@uhu.es (J.P. Bolívar).

the need for in-depth radiochemical studies prior to the search for future applications. During the chemical attack of the phosphate rock, the impurities are partitioned according to their respective elementary chemical behaviours. Between 85% and 95% of most of the trace elements, including uranium and thorium, goes into the phosphoric acid fraction (liquid fraction), and therefore into the phosphate fertiliser, whether no purification processes are applied to remove these impurities. Conversely, more than half of the Sr and Y content and radium-isotopes such as ^{210}Pb and ^{210}Po co-precipitate with the PG since they are chemically very similar to calcium (Pérez-López et al., 2010; Bolívar et al., 2009b; Mazzilli et al., 2000). The concentration of some impurities in the PG, such as P_2O_5, Cd or Y, has been found to exceed that of the typical uncontaminated soils, but others, such as Cr or Pb, have been observed to fall below uncontaminated typical soils (Pérez-López et al., 2010; Rudnick and Gao, 2003). Nevertheless, these results may vary significantly depending on the phosphate rock origin (Tayibi et al., 2009).

Despite these drawbacks, environmentally friendly applications are already being investigated. One of them is based on the use of PG as a calcium source for CO_2 mineral sequestration in the framework of the mitigation of greenhouse gasses emissions. It is well known that some calcium-rich compounds can be considered as efficient sinks of carbon dioxide by carbonation reactions. Mineral sequestration is a promising strategy for permanently fix carbon dioxide (Seifritz, 1990; Power et al., 2013) which involves a naturally occurring reaction in geological formations where aqueous ions (mainly Ca and Mg resulting from silicates or oxides) react with CO_2 to form stable carbonate minerals. The speed of the reaction and the costs associated with the scale-up from laboratory to industry are the major drawbacks of this technology. However, this carbonation reaction can be accelerated by using sequester agents with high specific surface areas (Santos et al., 2009) and the costs could be reduced by using industrial alkaline wastes (Kirchofer et al., 2013) as Ca and Mg sources, e.g. municipal solid waste bottom-ash (Rendek et al., 2006), paper mill wastes (Pérez-López et al., 2008) or coal combustion fly-ash (Montes-Hernandez et al., 2009). Moreover, neither high pressure nor high temperature are needed because some waste slurries, such as acetylene production wastes (Morales-Flórez et al., 2011), are able to capture CO_2 in very soft conditions, even at atmospheric concentrations. In addition, mineral sequestration is able to fix not only carbon dioxide from localised sources but also that from diffuse pollution sources such as road traffic and past emissions.

In this context, a recent work has offered the first approach to the use of phosphogypsum wastes as a Ca source for carbon dioxide mineral sequestration (Cárdenas-Escudero et al., 2011). It reports the very high efficiency of the process and the behaviour of the main metals; however, as far as we know, no thorough study concerning fractionation and flow of trace metals and radionuclides throughout the complete carbonation process using phosphogypsum has been conducted. To bridge this information gap, the present study focuses on the characterisation of the contents of metallic impurities and radionuclides in raw materials and products during the complete procedure. The obtained results provide very useful information which should help with the development of technological solutions to this environmental problem.

2. Materials and methods

2.1. Phosphogypsum sampling and pretreatment

After preliminary characterisation of the phosphogypsum stacks in Huelva (Renteria-Villalobos et al., 2010), a representative sample was collected ($\approx$2 kg at 0–15 cm depth). To develop the chemical, mineralogical and radioactive characterisation an aliquot of the original PG sample was dried at 60 °C until it reached constant weight, ground and homogenised in a planetary mill at 400 rpm for 20 min. Drying at 60 °C removes free water from the sample without losing structural water in gypsum.

2.2. Experimental carbonation procedure

The experimental carbonation procedure was made using the original PG material, in order to reproduce it under real conditions. The process can be conceptually divided into two steps: (a) PG dissolution, and (b) subsequent carbon sequestration. In Fig. 1, the entire experimental procedure is sketched; full details of the methodology can be found elsewhere (Cárdenas-Escudero et al., 2011). The first process started with the dispersion of PG in distilled water at room pressure and temperature with a PG/H_2O mass ratio of four, and then NaOH (pellets PA-ACS-ISO, PANREAC Química SAU, 98% chemical purity) was added to reach an OH^-/Ca^{2+} molar ratio of two under constant magnetic stirring for 3 h. The chemical reaction of this first step can be written as:

$$CaSO_4 \cdot 2H_2O + 2NaOH \leftrightarrow Ca(OH)_2 + Na_2SO_4 + 2H_2O \qquad (2)$$
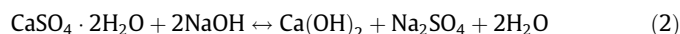
This procedure resulted in the PG's dissolution and the precipitation of a whitish solid phase labelled 'S1', ($Ca(OH)_2$, Eq. (2)) and a transparent supernatant liquid labelled 'L1'. The S1 was obtained by filtration, and the L1 was evaporated to dryness on a hot plate, yielding transparent salts labelled 'S2' (Na_2SO_4, Eq. (2)).

The second process began with the dispersion of sample S1 in distilled water under magnetic stirring in a reactor with a $S1/H_2O$ mass ratio of 1/20. A CO_2 flux ($\sim$1 bar, 20 cm^3 s^{-1}) was bubbled through the suspension for 15 min at room pressure and temperature. Afterwards, the sample was left to rest overnight in the CO_2-rich water. The carbonation reaction can be written as:

$$Ca(OH)_2 + CO_2 \leftrightarrow CaCO_3 + H_2O \qquad (3)$$

The resulting solid phase labelled 'S3' ($CaCO_3$, Eq. (3)) was separated by centrifugation and dried in air at 80 °C. The supernatant was labelled 'L2'. It was evaporated to dryness, yielding a precipitate labelled 'S4'. The carbonation experiments were repeated five times so their reproducibility could be analysed and uncertainties associated with the experimental procedure evaluated.

2.3. Analytical techniques

The mineral characterisation of the raw materials (PG and sodium hydroxide) and the final solid products was performed by X-ray diffraction (XRD, powder method) with a Bruker diffractometer (D8-Advance with Cu Kα radiation). Diffractometer settings were 40 kV, 30 mA, a scan range of 3–65° (2θ) with a step size of 0.02° and a counting time of 0.6 s per step. Analysis of diffraction patterns was performed with the XPowder software (Martín-Ramos, 2004). By using the original PG sample, the particle size analysis was performed by laser granulometry in wet suspensions with water as dispersant, using a Malbern Mastersizer 2000 particle sizer with Hydro 2000 M accessory. Furthermore, morphological analyses of the samples were obtained by the use of a JEOL JSM 5410 scanning electron microscope (SEM) working at 20 kV.

Major elements were analysed by X-ray fluorescence (XRF) with a Bruker spectrometer S4 Pioneer equipped with an X-ray tube of 4 kW (front window), anode of Rh, five analyser crystals (LIF200, Ge, PET, OVO 55 and OVO C) and both flow and scintillation detectors. Trace elements were determined by ICP-MS (inductively coupled plasma mass spectrometry) after four-acid digestion at the Activation Laboratories Ltd (ACTLABS, Ontario, Canada), which meet the ISO/IEC 17025 Quality System standard. The quality control method included the use of a reagent blank, standard reference
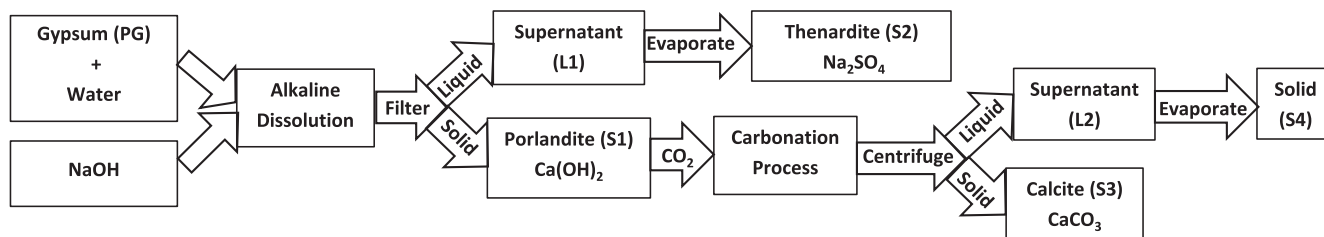
Fig. 1. Diagram of the experimental methodology.

materials and replicates. The average accuracy of the analytical data was ±5%.

The carbonate concentration and carbonation degree of the samples was studied by thermogravimetric analysis (TGA; STD Q600) carried out under a nitrogen flux of 100 mL/min, starting from ambient temperature and increasing by 10 °C/min up to 1000 °C. The carbonation degree of samples was estimated by comparing measured weight losses between 500 °C and 900 °C with the stoichiometric weight loss of pure calcite within this range due to decarbonation (44%). To compare the experimental results with this theoretical maximum, the mass of the samples was normalised to the measured weight at 200 °C and the mass of possible impurities was also considered.

The activity concentrations of natural radionuclides were measured by both alpha-particle spectrometry and high-resolution low-background gamma spectrometry with a hyper-pure germanium detector with a carbon window. Thorium and uranium isotopes were determined by applying the alpha spectrometry technique with ion-implanted Si detectors, and U, Th and ^{210}Po were isolated by the tributilphosphate method. Detailed information about the characterisation techniques is available in the literature (Lozano et al., 2011). Activity concentrations of the gamma emitters were measured through the following energies: ^{210}Pb (46.5 keV), ^{234}Th (63.3 keV), ^{226}Ra (352 keV of ^{214}Pb) and ^{40}K (1460 keV).

3. Results and discussion

3.1. Materials

3.1.1. Starting materials

The mineralogical analysis confirmed the exclusive presence of gypsum in the raw *PG* sample (see XRD pattern of Fig. 2). In addition, its elemental composition, shown in Table 1, indicates that *PG* is mainly composed of S (51.5 wt.% as SO_3) and Ca (36.6 wt.% as CaO). These results are similar to those reported in other studies (Martín et al., 1999; Arocena et al., 1995) and correspond to a molar ratio of Ca/S = 1.015 ± 0.005, very close to the expected molar ratio of gypsum, Ca/S ∼1. The main impurities of the *PG* are F (2.2 wt.%), P (0.3 wt.% as P_2O_5), Si (0.6 wt.% as SiO_2) and Al (0.18 wt.% as Al_2O_3). The results of the particle size analysis of phosphogypsum, determined by laser granulometry, are shown in Fig. 3. The granulometric profile of *PG* revealed that the sample presented a wide range of particles sizes, with an asymmetric distribution of particles. The slope of the granulometric curve denotes almost two populations of particles with a large particle size range. The first population has a significant particle number of around 3.5 μm of diameter. The intermediate fraction is the greatest fraction in this sample; most of the particle distribution in *PG* was detected by laser above 50 μm. SEM observations reveal the presence of gypsum crystals that occur as well-developed euhedral monoclinic laths with tabular habit between 40 and 100 μm long (Fig. 4), according particle size distribution analysis. The main trace
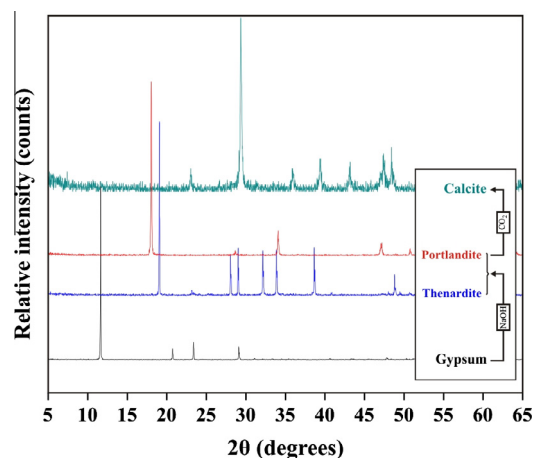

Fig. 2. XRD patterns super-impose of *PG* (gypsum), *S1* (portlandite), *S2* (thenardite) and *S3* (calcite).

elements identified in the *PG* are Sr, Y, La, Cr, Cu and Zn, in order of abundance. Some trace elements (Cr, Cu, Zn, V, Pb, As and Ag) are present in concentrations smaller than uncontaminated soils, but others, such as Cd, Y, Se, La and Sr, are higher (Contreras et al., 2014). Regarding the sodium hydroxide reagent, some trace impurities such as K, Ni, Mn, Cr, Cu, As and Zn were detected, all of them typically below 2 mg kg^{-1}.

3.1.2. Materials from PG dissolution process

$$PG\ (1.00\,g) + NaOH\ (0.47\,g) \leftrightarrow S1\ (0.49\,g) + S2\ (0.94\,g) \qquad (4)$$
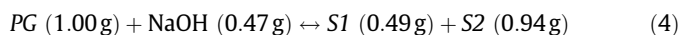
PG dissolution resulted in the precipitate *S1* and in a transparent supernatant, *L1*. The composition of *L1* was analysed through the precipitate obtained by evaporation (sample *S2*). The XRD patterns (Fig. 2) reveal only the presence of portlandite and thenardite in samples *S1* and *S2*, respectively, according to the reaction (Eq. (2)). In addition, in Table 1, the major elements of the different samples measured by XRF are listed. Sample *S1* was mainly composed of Ca (73.3 wt.%) in coherence with the observed portlandite in the XRD pattern. In addition, there are also certain amounts of Na (3.4 wt.% as Na_2O) and S (5.6 wt.%), which indicate the likely presence of 9 wt.% of residual thenardite in the sample, as the result of incomplete phase separation, and it could easily be removed by rinsing. Minor reflections in the XRD patterns of replicas of *S1* (not indicated in Fig. 2) support this assumption. Again, minor F, Si and P contents (2.2 wt.%, 0.9 wt.% and 0.7 wt.%, respectively) are noteworthy in *S1* as they suggest the presence of the impurities derived from the starting *PG* sample. TGA analysis (Fig. 5) showed a weight loss at 400 °C that is characteristic of the dehydration of portlandite. The measured weight loss covers 20.3 ± 0.9 wt.%, as expected for a portlandite sample with 9 wt.% of impurities.

Table 1
Average concentrations ($n = 6$) of major elements (wt.%) and trace elements (mg kg^{-1}) in the experimental process. Phosphogypsum (PG), portlandite (S1), thenardite (S2), calcite (S3) and dry solid residue coming from final liquid fraction (S4). (*) Continental crust composition [12]. Uncertainties given as standard deviation of the mean: $u = (S_x/n^{1/2})$, being S_x the standard deviation of the samples. Major elements measured by XRF and trace elements measured by ICP-MS.

|	Raw materials			Alkaline dissolution ($PG + NaOH \rightarrow S1 + S2$)			Carbonation Process ($S1 + CO_2 \rightarrow S3 + S4$)			Soil (*)
	PG (1.00 g)	+	NaOH (0.47 g)	S1 (0.49 g)	+	S2 (0.94 g)	S3 (0.50 g)	+	S4 (0.022 g)	
Major elements										
CaO	36.6 ± 0.1		<0.01	73.3 ± 0.9		0.7 ± 0.2	59.4 ± 0.5		13.8 ± 7.5	3.44
Al$_2$O$_3$	0.184 ± 0.002		<0.01	0.31 ± 0.02		<0.01	0.25 ± 0.01		<0.01	14.17
SO$_3$	51.53 ± 0.25		<0.01	5.6 ± 0.8		38 ± 8	4.8 ± 0.9		<0.01	–
P$_2$O$_5$	0.328 ± 0.006		<0.01	0.668 ± 0.008		<0.01	0.57 ± 0.04		<0.01	0.16
K$_2$O	0.030 ± 0.001		0.031 ± 0.001	0.040 ± 0.002		0.031 ± 0.005	0.04 ± 0.01		<0.01	2.68
Na$_2$O	0.13 ± 0.03		98 ± 1	3.4 ± 0.4		45 ± 6	2.5 ± 0.9		40.5 ± 1.8	2.86
SiO$_2$	0.61 ± 0.01		<0.01	0.86 ± 0.01		1.0 ± 0.1	0.7 ± 0.1		<0.01	–
Trace elements										
Sr	435 ± 37		<0.1	611 ± 55		115 ± 16	476 ± 4		<0.1	348
Y	79 ± 3		<0.1	152 ± 15		<0.1	130 ± 12		<0.10	21
Cd	0.7 ± 0.1		<0.1	1.7 ± 0.1		<0.1	1.65 ± 0.07		<0.1	0.09
V	4.5 ± 0.7		<0.1	7.0 ± 0.1		<0.1	6.0 ± 0.1		8.5 ± 0.7	97
Cr	10.8 ± 2.0		2.2 ± 0.5	25.3 ± 5.0		5.0 ± 0.1	19.1 ± 0.6		9.3 ± 3.4	92
Ag	0.66 ± 0.01		0.17 ± 0.01	1.4 ± 0.1		0.15 ± 0.08	1.3 ± 0.1		0.22 ± 0.09	65
Se	3.8 ± 0.8		<0.1	7.1 ± 0.2		0.75 ± 0.07	6.7 ± 0.1		2.3 ± 0.4	0.09
Zn	7.6 ± 1.1		1.0 ± 0.1	11.6 ± 1.1		3.15 ± 0.07	13.0 ± 2.5		36.6 ± 46.5	67
As	1.9 ± 0.4		0.30 ± 0.02	3.2 ± 0.1		0.6 ± 0.1	2.9 ± 0.1		1.85 ± 0.21	4.8
La	35.5 ± 9.1		<0.1	87.7 ± 0.7		0.2 ± 0.1	100 ± 6		<0.1	17
Pb	4.1 ± 0.7		<0.5	9.7 ± 0.4		<0.5	10.2 ± 0.5		<0.5	17
Cu	8.4 ± 0.6		1.3 ± 0.3	11.7 ± 0.3		2.8 ± 0.3	11.1 ± 0.8		1.9 ± 0.7	28
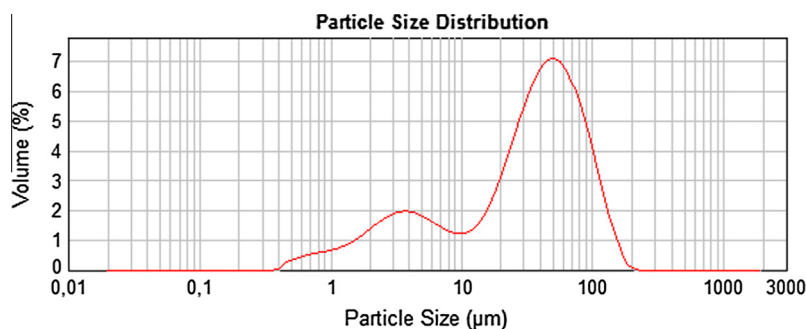
Fig. 3. Granulometric range curve of phosphogypsum.

On the other hand, sample S2 was mainly dominated by Na (45.3 wt.%) and S (50.8 wt.%). These major elements indicate a composition close to pure thenardite (Na_2SO_4), as expected from the XRD pattern (Fig. 2). The presence of CaO in S2 is very low (<0.7 wt.%), indicating that the calcium from the initial PG sample was almost completely transferred to sample S1.

Finally, as observed by SEM, S1 showed a hexagonal-platy habit up to 25 µm across typically observed in portlandite samples; thenardite aggregates in sample S2 occurred as prismatic-shaped crystals up to 200 µm (Fig. 4).

3.1.3. Materials from carbonation process

$$S1\ (0.49\,g) + CO_2\ (0.26\,g) \leftrightarrow S3\ (0.50\,g) + S4\ (0.022\,g) \qquad (5)$$
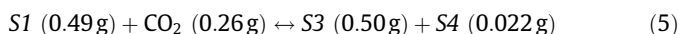
The aqueous carbonation of sample S1 (portlandite) upon CO$_2$ injection in aqueous media, following the reaction of Eq. (3), produced a solid precipitate S3 that showed a high content of Ca (59.4 wt.%, Table 1), slightly higher than the stoichiometric content of calcite, probably because of the transference of the residual calcium-bearing impurities present in sample S1. The XRD analyses of this sample revealed the disappearance of portlandite and the presence only of calcite (Fig. 2), confirming therefore the complete carbonation of sample S1. In addition, the TGA analysis (Fig. 5)

showed the presence of a weight loss around 37 ± 1% at $T = 700\ °C$, a characteristic value from decarbonation of calcite with less than 10 wt.% of impurities, similarly to what was described before for sample S1. SEM images revealed that the newly-formed calcite morphology occurred as agglomerates of fine-grained powder (Fig. 4).

With regard to sample S4, which was obtained upon evaporation of the supernatant after the aqueous carbonation L2, it was mainly composed of Na and Ca (40.5 wt.% and 13.8 wt.%, respectively; Table 1), the Na content probably deriving from the non-separated rests of thenardite contained in S1 which were subsequently transferred to solution during the carbonation step. It should be noted that the mass of the solid S4 obtained was around 0.022 g per gram of PG, and this fraction is negligible in relation to the total amount of Na and Ca involved in the overall process.

3.2. Partitioning and fluxes of major and trace elements

To study the partitioning of elements during the dissolution and carbonation processes, a transfer factor (η) was defined, which represents the fraction of each element that remains in each one of the products in relation to the initial input of all the reactants and is given by the following equation:
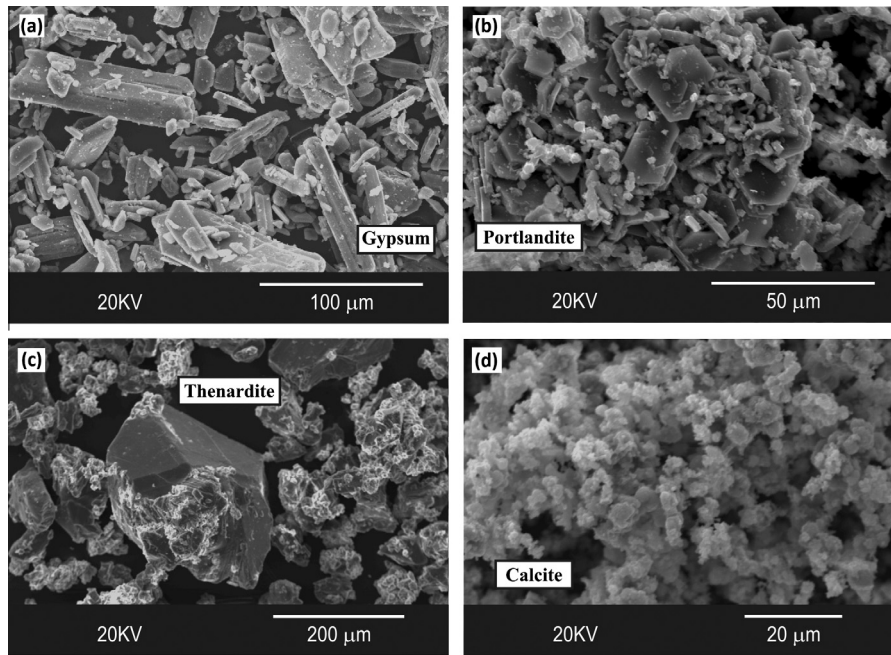
Fig. 4. SEM microphotographs of samples produced in the present work: (a) *PG* (gypsum); (b) *S1* (portlandite); (c) *S2* (thenardite) and (d) *S3* (calcite).
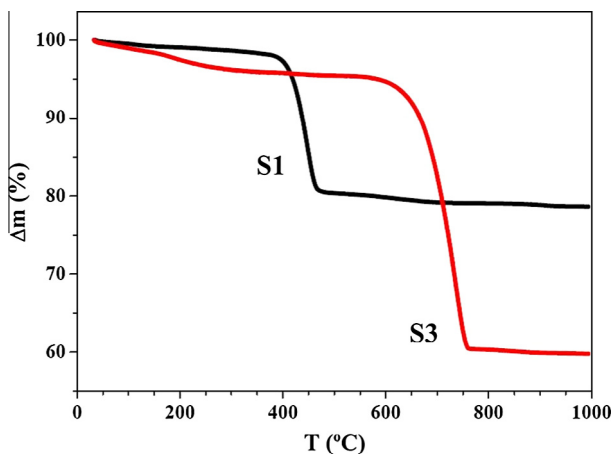

Fig. 5. TGA of samples *S1* (portlandite) and *S3* (calcite).

$$\eta_i(\%) = \frac{C_{Pi} \times f_{Pi}}{\sum C_{Ri} \times f_{Ri}} \times 100 \qquad (6)$$

where C_{Pi} and C_{Ri} are the concentrations of the element of interest in the products and reactants for each reaction of the carbon mineral sequestration process, f being the 'mass factor' of each reactant, i.e. the experimentally involved mass in the chemical reaction for each reactive added (R_i) or each product generated (P_i).

The values of the mass factors (f) were experimentally measured by repeating the procedure five times, achieving these values (Eqs. (4) and (5)): 1.00 (reference, *PG*), 0.47 (NaOH), 0.49 ± 0.09 (portlandite, *S1*), 0.94 ± 0.05 (thenardite, *S2*), 0.50 ± 0.08 (calcite, *S3*) and 0.022 ± 0.005 (final dry solid residue from evaporation of the final liquid fraction, *S4*). Table 2 shows the transfer factor (η) of major elements measured by XRF and trace elements measured by ICP-MS in the products resulting from the overall process.

The process of *PG* dissolution and carbonation can be traced through the major elements Ca and S. According to the XRD and XRF data, 97% of Ca was transferred from the *PG* to the *S1* and

95% from *S1* to *S3*. On the other hand, most of the S (>95%) in the *PG* was partitioned, along with Na from sodium hydroxide, into the *S2*. Other elements such as Al, Y, S and P were also completely transferred to the portlandite and on subsequent carbonation to the calcite (Table 2). As regards the trace impurities initially contained in the *PG*, most of these elements were also found to have been completely transferred to the final calcite.

Thus, the concentrations in the *S1* and *S3* implied high transfer factors, with average values for the trace elements of 90% and 98%, respectively (Table 2). Logically, the dissolution of phosphogypsum and precipitation of portlandite/calcite implies a loss of mass and, therefore, an increase effect in the concentration of contaminants. Similarly to the precursor phosphogypsum, the elements with higher concentrations than uncontaminated soils in *S1* (portlandite) and *S3* (calcite) continue to be Sr, Y, Cd, Se and La (Table 1). On the other hand, in samples *S2* and *S4*, most contaminants are in lower concentrations compared with their corresponding solids (*S1* and *S3*, respectively), with some values close to or even below the detection limit. It is worth noting relatively high transfer factors for Cr (40%), Zn (36%), Cu (29%), As (28%) and Sr (25%) in *S2*, and Zn (14%) in *S4*. However, Se is the only element which is slightly above the concentrations of uncontaminated soils in all the samples (Contreras et al., 2014). Moreover, the final dry solid residue (*S4*) showed negligible values, barely taking part in the transfer fluxes, because of the small quantity of sample obtained.

3.3. Radioactive characterisation and fluxes of radionuclides

Phosphate rock used in the factory of Huelva contains U- and Th-series radionuclides in secular equilibrium (1600 and 15 Bq kg^{-1} of ^{238}U and ^{232}Th series, respectively) (Bolivar et al., 1996, 1995). Considering the differences in activity concentrations measured for the radionuclides with high half-life (>one year, ^{238}U, ^{230}Th, ^{226}Ra and ^{232}Th), the secular equilibrium is broken during the industrial process of phosphoric acid production. The radionuclides contained in the phosphate rock are distributed between *PG* (U-series) and phosphoric acid, depending on their solubility and

Table 2
Transfer factor (η) defined as the mass (g) of products for every g of phosphogypsum that reacts during the carbonation process. Phosphogypsum (PG), Portlandite (S1), Thenardite (S2) Calcite (S3) and solid residue from the evaporation of final liquid fraction (S4).

	Raw materials			Alkaline dissolution ($PG + NaOH \rightarrow S1 + S2$)			Carbonation process ($S1 + CO_2 \rightarrow S3 + S4$)		
	PG	+	NaOH	S1	+	S2	S3	+	S4
Major elements									
CaO	100		<0.1	97.4		1.8	84.8		1.3
Al_2O_3	100		<0.1	80.9		10.2	84.0		<0.1
SO_3	100		<0.1	5.9		98.1	78.4		<0.1
P_2O_5	100		<0.1	98.8		<0.1	88.4		<0.1
K_2O	68.0		32.0	33.3		79.9	102		5.6
Na_2O	0.2		99.8	3.6		92.6	59.3		53.8
Trace elements									
Sr	100		<0.1	68.2		24.8	96.5		3.4
Y	100		<0.1	93.7		<0.1	87.8		<0.1
Cd	100		<0.1	118.0		<0.1	99.9		<0.1
V	100		<0.1	75.6		<0.1	88.2		5.5
Cr	100		<0.1	104.2		39.9	77.6		1.7
Ag	100		<0.1	90.7		18.3	92.5		0.7
Se	100		<0.1	91.4		18.8	97.8		1.5
Zn	94.2		5.7	69.4		36.4	115.3		14.3
As	93.12		6.88	76.2		27.6	94.8		2.6
La	100		<0.1	120.2		0.5	117.3		<0.1
Pb	100		<0.1	115.0		<0.1	108.7		<0.1
Cu	100		<0.1	63.1		29.2	97.2		0.7

chemical affinity (Rutherford et al., 1996; Abril et al., 2009), as stated before.

The homogenised *PG* sample used in the carbonation experiments contains 670 ± 36 Bq kg^{-1} of ^{226}Ra (Table 3), which is in agreement with previous works (Mazzilli et al., 2000; Carvalho, 2001). Similar conclusions were obtained for the rest of the radionuclides (^{238}U, ^{230}Th and ^{210}Pb–^{210}Po). Particularly striking is the behaviour of the ^{226}Ra, with a concentration around 700 Bq kg^{-1} (considered as NORM material), which exceeds the upper limit set by the USEPA (370 Bq kg^{-1}) for use as a soil amendment (NES, 1992; IAEA, 2004). Other radionuclides have activity concentrations slightly smaller than ^{226}Ra, such as ^{230}Th (502 ± 42 Bq kg^{-1}) and ^{210}Pb (554 ± 32 Bq kg^{-1}). On the other hand, the concentrations of U-isotopes were very much lower than the rest of the U-series radionuclides (68 ± 8 Bq kg^{-1} of ^{238}U), as expected, since the solubility of U is very high in acid media, and more than 85% remains in the phosphoric acid fraction during the chemical industrial process. Finally, Th-series radionuclides present very low levels in *PG*, being generally near or below the detection limit (around 1 Bq kg^{-1}).

The radionuclides concentrations in the different products of the dissolution and carbonation are shown in Table 3. In general, it can be observed that the majority of the radionuclides initially present in *PG* accumulate in the different products containing the calcium (S1 and S3); and the concentrations of U-isotopes, Ra-isotopes and Th-isotopes in S1 (portlandite) and S3 (calcite) are twice as high as in the raw material (*PG*), being around 1100, 130, 1400 and 900 Bq kg^{-1} for ^{210}Pb–^{210}Po, ^{238}U, ^{226}Ra and ^{230}Th, respectively. According to the European Union regulation, S1 and S3 are NORM materials, and therefore radiological control has to be applied during their commercial application. On the other hand, the radionuclides' concentrations in S2 (thenardite) are lower than in uncontaminated soils (Contreras et al., 2013).

The transfer factors involved during the complete process are also shown in Table 3, and as a general conclusion it can be stated that 95% of the radionuclides' activity was transferred during the dissolution reaction to the portlandite. Because of the chemical affinity between Ca and Ra, these two elements have similar behaviour during the experimental run (Haridasan et al., 2001). Concentrations in S1 and S3 increase up to twofold because

Table 3
Summary of reported average activity concentrations ($n = 6$), of radionuclides studied (Bq kg^{-1} dry weight) from phosphogypsum (PG), Portlandite (S1), Thenardite (S2) and Calcite (S3). Transfer factor (%) in the experimental process is also shown. Uncertainties given as standard deviation of the mean. Radionuclides were not measured in S4 due to the low amount obtained of this fraction.

|		Raw materials			Alkaline dissolution			Carbonation
		PG	+	NaOH	S1	+	S2	S3
^{210}Pb/^{210}Po	C (Bq kg^{-1})	554 ± 32		<0.2	1104 ± 38		21 ± 6	1124 ± 84
	η (%)				96.7		3.6	104.7
^{234}Th	C (Bq kg^{-1})	63.5 ± 7		<0.2	118 ± 8		<3.2	114 ± 9
	η (%)				90.0		<0.1	99.5
^{232}Th	C (Bq kg^{-1})	7.5 ± 0.5		<0.2	16 ± 1		<2.2	16 ± 3
	η (%)				92.5		<0.1	100.8
^{230}Th	C (Bq kg^{-1})	502 ± 42		<0.2	946 ± 30		12 ± 11	853 ± 25
	η (%)				88.1		2.2	92.8
^{226}Ra (^{214}Pb)	C (Bq kg^{-1})	670 ± 36		<0.2	1451 ± 64		<9.2	1420 ± 90
	η (%)				101.2		<0.1	100.7
^{238}U	C (Bq kg^{-1})	68 ± 8		<0.2	143 ± 7		1.5 ± 0.6	128 ± 3
	η (%)				102.4		2.1	91.9
^{40}K	C (Bq kg^{-1})	<18		<15	<20		<16	<15
	η (%)	–		–	–		–	–

impurities contained in the starting phosphogypsum are transferred to the products and only half of weight of products is generated according to the stoichiometry of both reactions. The thenardite contains very low levels of radionuclides, the activity concentrations being near to the detection limits. After the carbonation process, the majority of the natural radioactivity contained in *PG* is transferred to calcite (98%). The radionuclides' concentrations in the dissolution and carbonation liquid phases (supernatants *L1* and *L2*, respectively) were in all cases below the detection limits of the analytical techniques, and so they are not shown in Table 3.

3.4. Environmental implications

The gypsum by-product contains a residual fraction of free acids, mainly H_3PO_4, H_2SO_4 and HF, which come from the industrial process (see Eq. (1)). H_3PO_4 is the main residual acid and corresponds to the fraction of acid that is not effectively separated in the industry to be commercialised for fertiliser manufacture. Most of the toxic impurities in the phosphogypsum stack are mobile and are concentrated in the acid solutions occupying the interstitial pore spaces. These highly-polluted acidic solutions certainly represent the true environmental danger of the phosphogypsum stack because the dump is not totally watertight and some groundwater can migrate laterally to reach the estuary of Huelva (Bolívar et al., 1995). In fact, these effluents leave their characteristic radioactive fingerprint on the estuarine water and sediments, and may even extend to remote areas as a result of tidal action (Pérez-López et al., 2010).

In the experimental protocol proposed in this study, most of these pollutants, i.e. phosphorus as indicative of H_3PO_4, metals and radionuclides (Tables 1 and 2), are put into solution during the dissolution of phosphogypsum and removed satisfactorily into the stable final solids. Therefore, this procedure would not only help to mitigate local emissions of CO_2 to the atmosphere but could also reduce the potential risk of pollution from the phosphogypsum stack to the estuarine environment.

According to the results, the carbon dioxide capture by phosphogypsum is a sustainable and environmental-oriented procedure to manage this waste.

$$CaSO_4 \cdot 2H_2O + 2NaOH + CO_2 \leftrightarrow CaCO_3 + Na_2SO_4 + 2H_2O \qquad (7)$$
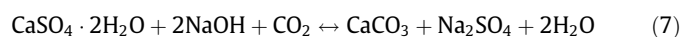
The sequestration capacity of the phosphogypsum has been measured experimentally, finding that the following amounts of reactants and products are involved for each gram (1 g) of waste in the overall reaction: 0.47 g of NaOH, 0.26 g of CO_2, 0.84 g of Na_2SO_4 and 0.50 g of $CaCO_3$. (Eq. (7)). Based on these experimental results, the carbon capture capacity of the stockpiled phosphogypsum waste is around 30 Mt of CO_2 since in the repository there are stored about 120 Mt of phosphogypsum.

4. Conclusions

The research on fractionation and fluxes of hazardous impurities throughout the CO_2 mineral sequestration process by phosphogypsum wastes resulted in one major conclusion. Most of the trace metals and radionuclides were transferred from the initial raw waste to the portlandite after phosphogypsum dissolution, and then to the calcite after carbonation reaction. In particular, 97% of the Ca in the phosphogypsum was transferred to the portlandite by alkaline dissolution, which subsequently achieved almost complete carbonation after CO_2-bubbling in aqueous media. Other elements such as Al, Y, S and P behaved in a similar fashion. Thus, this work confirmed that the carbonation potential of the phosphogypsum stacks in SW Spain can be estimated at

~30 Mt of CO_2, and the estimated worldwide phosphogypsum production would be able to capture 70 Mt of carbon dioxide per year.

In addition, the concentrations in the portlandite and calcite of most of the trace impurities initially contained in the *PG* implied average transfer factors of 100%, so most of these elements would be fixed in this final calcite, some being present in concentrations above those typical of uncontaminated soils, such as Se, Sr, Cd, Y and La, as in the raw *PG*. Conversely, almost no contaminants remained in the thenardite solution resulting from the *PG* dissolution which exceeded the concentration of uncontaminated soils, except Se.

Finally, the radionuclides present in the original wastes ^{226}Ra, ^{238}U, ^{230}Th and ^{210}Pb–^{210}Po were almost completely transferred to the intermediate portlandite on the dissolution of *PG*, and also to the final calcium carbonate sample after the carbonation process. In particular, the most important radionuclide present in the *PG*, ^{226}Ra, behaves similarly to Ca throughout the process because of their chemical affinity. According to the EU regulations, these portlandite and calcite samples are NORM materials and should be controlled for any commercial application. Conversely, the liquid phases of the dissolution process (thenardite solution) and the carbonation process were free of these contaminants.

The simple process proposed in this work will not only deal with carbon dioxide but also reduce the mobility of trace metals and toxic contaminants, reducing their transference from the phosphogypsum stacks to the environment.

References

Abril, J.M., García-Tenorio, R., Manjón, G., 2009. Extensive radioactive characterization of a phosphogypsum stack in SW Spain: ^{226}Ra, ^{238}U, ^{210}Po concentrations and ^{222}Rn exhalation rate. J. Hazard. Mater. 164, 790–797.

Arocena, J.M., Rutherford, P.M., Dudas, M.J., 1995. Heterogeneous distribution of trace elements and fluorine in phosphogypsum by-product. Sci. Total Environ. 162, 149–160.

Bolívar, J.P., Martín, J.E., García-Tenorio, R., Pérez-Moreno, J.P., Mas, J.L., 2009a. Behaviour and fluxes of natural radionuclides in the production process of a phosphoric acid plant. Appl. Radiat. Isot. 67, 345–356.

Bolívar, J.P., Pérez-Moreno, J.P., Mas, J.L., Martín, J.E., San Miguel, E.G., García-Tenorio, R., 2009b. External radiation assessment in a wet phosphoric acid production plant. Appl. Radiat. Isotopes 67, 1930–1938.

Bolivar, J.P., García-Tenorio, R., Garcia-Leon, M., 1996. On the fractionation of natural radioactivity in the production of phosphoric acid by the wet acid method. J. Radioanal. Nucl. Chem. 214, 77–78.

Bolivar, J.P., García-Tenorio, R., Garcia-Leon, M., 1995. Fluxes and distribution of natural radionuclides in the production and use of fertilizers. Appl. Radiat. Isot. 46, 717–718.

Bolívar, J.P., García-Tenorio, R., García-León, M., 1995. Enhancement of natural radioactivity in soils and salt-marshes surrounding a non-nuclear industrial complex. Sci. Total Environ. 173, 125–135.

Cárdenas-Escudero, C., Morales-Flórez, V., Pérez-López, R., Santos, A., Esquivias, L., 2011. Procedure to use phosphogypsum industrial waste for mineral CO_2 sequestration. J. Hazard. Mater. 196, 431–435.

Carvalho, F.P., 2001. Disposal of phosphogypsum waste containing enhanced levels of radioactivity, International conference on management of radioactive waste from non-power applications – Sharing the experience, 5–9 November 2001. Book of extended synopses. IAEA-CN-87/6, pp. 67–68.

Contreras, M., Martín, M.I., Gázquez, M.J., Romero, M., Bolívar, J.P., 2014. Valorisation of ilmenite mud waste in the manufacture of commercial ceramic. Constr. Build. Mater. 72, 31–40.

Contreras, M., Gázquez, M.J., García-Díaz, I., Alguacil, F.J., López, F.A., Bolívar, J.P., 2013. Valorisation of waste ilmenite mud in the manufacture of sulphur polymer cement. J. Environ. Manage. 128, 625–630.

Haridasan, P.P., Paul, A.C., Desai, M.V.M., 2001. Natural radionuclides in the aquatic environment of a phosphogypsum disposal area. J. Environ. Radioact. 53, 155–165.

IAEA (International Atomic Energy Agency), Application of the concepts of exclusion exemption and clearance. Safety standards series, Safety guide no RS-G 17 August 2004, STI/PUB/1202.

Kim, G.H., 2010. A study on establishing quality certification of standardization for waste gypsum recycling. Final report, Incheon (Korea): Korea Environment Corporation (Korea), Division of research and development. Report No.: KECO2010-RE17-31. Contract No.: 11-1480000-001132-01.

Kirchofer, A., Becker, A., Brandt, A., Wilcox, J., 2013. CO_2 mitigation potential of mineral carbonation with industrial alkalinity sources in the United States. Environ. Sci. Technol. 47, 7548–7554.

Lozano, R.L., Bolívar, J.P., San Miguel, E.G., García-Tenorio, R., Gázquez, M.J., 2011. An accurate method to measure alpha-emitting natural radionuclides in atmospheric filters: application in two NORM industries. Nucl. Instrum. Method A 659, 557–568.

Martín, J.E., García-Tenorio, R., Respaldiza, M.A., Ontalba, M.A., Bolívar, J.P., da Silva, M.F., 1999. TTPIXE analysis of phosphate rocks and phosphogypsum. Appl. Radiat. Isot. 50, 445–449.

Martín-Ramos, J.D., 2004. Using XPowder: a software package for powder X-ray diffraction analysis, D.L. GR-1001/04 84-609-1497-6, Spain, <http://www.xpowder.com> (accessed 09.06.14).

Mas, J.L., San Miguel, E.G., Bolívar, J.P., Vaca, F., Pérez-Moreno, J.P., 2006. An assay on the effect of preliminary restoration tasks applied to a large TENORM wastes disposal in the south-west of Spain. Sci. Total Environ. 364, 55–66.

Mazzilli, B., Palmiro, V., Saueia, C., Nisti, M.B., 2000a. Radiochemical characterization of Brazilian phosphogypsum. J. Environ. Radioact. 49, 113–122.

Mazzilli, B., Palmiro, V., Saueia, C., 2000b. Radiochemical characterization of Brazilian phosphogypsum. J. Environ. Radioact. 49, 113–122.

Montes-Hernandez, G., Pérez-López, R., Renard, F., Nieto, J.M., Charlet, L., 2009. Mineral sequestration of CO_2 by aqueous carbonation of coal combustion fly-ash. J. Hazard. Mater. 161, 1347–1354.

Morales-Flórez, V., Santos, A., Lemus, A., Esquivias, L., 2011. Artificial weathering pools of calcium-rich industrial waste for CO_2 sequestration. Chem. Eng. J. 166, 132–137.

N.E.S., 1992. National emission standards for hazardous air pollutants, national emission standards for radon emissions from phosphogypsum stacks, 40 CFR Part 61, Federal Register, U.S.A., vol. 57, no. 107, pp. 23305–23320.

Pérez-López, R., Nieto, J.M., López-Coto, I., Aguado, J.L., Bolívar, J.P., Santisteban, M., 2010. Dynamics of contaminants in phosphogypsum of the fertilizer industry of Huelva (SW Spain): from phosphate rock ore to the environment. Appl. Geochem. 25, 705–715.

Pérez-López, R., Montes-Hernández, G., Nieto, J.M., Renard, F., Charlet, L., 2008. Carbonation of alkaline paper mill waste to reduce CO_2 greenhouse gas emissions into the atmosphere. Appl. Geochem. 23, 2292–2300.

Pérez-López, R., Álvarez-Valero, A.M., Nieto, J.M., 2007. Changes in mobility of toxic elements during the production of phosphoric acid in the fertilizer industry of Huelva (SW Spain) and environmental impact of phosphogypsum wastes. J. Hazard. Mater. 148, 745–750.

Power, I.M., Harrison, A.L., Dipple, G.M., Wilson, S.A., Kelemen, P.B., Hitch, M., Southam, G., 2013. Carbon mineralization: from natural analogues to engineered systems. Rev. Mineral. Geochem. 77, 305–360.

Rendek, E., Ducom, G., Germain, P., 2006. Carbon dioxide sequestration in municipal solid waste incinerator (MSWI) bottom ash. J. Hazard. Mater. B128, 73–79.

Renteria-Villalobos, M., Vioque, I., Mantero, J., Manjón, G., 2010. Radiological, chemical and morphological characterizations of phosphate rock and phosphogypsum from phosphoric acid factories in SW Spain. J. Hazard. Mater. 181, 193–203.

Rudnick, R.L., Gao, S., 2003. Composition of the continental crust. In: Holland, H.D., Turekian, K.K. (Eds.), Treatise of Geochemistry, vol. 3. Elsevier, pp. 1–64.

Rutherford, P.M., Dudas, M.J., Arocena, J.M., 1996. Heterogeneous distribution of radionuclides, barium and strontium in phosphogypsum by-product. Sci. Total Environ. 180, 201–209.

Rutherford, P.M., Dudas, M.J., Samek, R.A., 1994. Environmental impacts of phosphogypsum. Sci. Total Environ. 149, 1–38.

Santos, A., Ajbary, M., Morales-Flórez, V., Kherbeche, A., Piñero, M., Esquivias, L., 2009. Larnite powders and larnite/silica aerogel composites as effective agents for CO_2 sequestration by carbonation. J. Hazard. Mater. 168, 1397–1403.

Seifritz, W., 1990. CO_2 disposal by means of silicates. Nature 345, 486.

Tayibi, H., Choura, M., López, F.A., Alguacil, F.J., López-Delgado, A., 2009. Environmental impact and management of phosphogypsum. J. Environ. Manage. 90, 2377–2386.

Yang, J., Liu, W., Zhang, L., Xiao, B., 2009. Preparation of load-bearing building materials from autoclaved phosphogypsum. Constr. Build. Mater. 23, 687–693.